Stress Sensitivity of Piezoelectric Ceramics: Part 1. Sensitivity to Compressive tress Parallel to the Polar Axis

HELMUT H. A. KRUTGER

Measurements of changes in permittivity, tanð, and d_{33} as function of compressive stress parallel to the polar axis are presented for lead zirconate-lead titanate transducer ceramics. The "hard" ceramics (PZT-4 and PZT-8) suitable for high-power application show large changes of properties for stresses to 20 kpsi, but have good recovery on release of stress. The "soft" donor-doped ceramics (PZT-5A and PZT-5H) suitable for detector applications show serious degradation with successive stress cycles. However, for peak stress below about 10 kpsi, their variation of properties and hysteresis within any cycle are less than those of the hard ceramics. Permittivity and tanð of all these ceramics increase with increase of ac electric field. For the soft ceramics, the tanð increase is great enough to eliminate their consideration for uses where efficiency or cool operation are necessary. High ac electric field combined with compressive stress reduces these detrimental increases for the soft ceramics and increases them for the hard ceramics. Nevertheless, the hard ceramics remain far superior for high-power high stress uses, with PZT-8 being superior to PZT-4.

INTRODUCTION

This paper is concerned with the power-handling A capability and sensitivity to static compressive stress of the piezoelectric ceramics used in underwater transducers. The electroelastic coefficients of the piezoelectric ceramics vary with the ambient static stress due to domain reorientation effects. Power-handling capacity is limited by the increase of dielectric and mechanical loss factors with increase in magnitude of the driving electric field and dynamic stress. These loss factors are also found to increase with static stress with materials used in radiating transducers. Proper use of piezoelectric ceramics in underwater transducers ref quires knowledge of these effects. In work reported here, permittivity and dielectric loss were measured as functions of static mechanical stress and combined stress and high ac driving fields. Piezoelectric d constants were also measured as a function of stress. Ceramics studied were PZT-4 and PZT-8, representative of materials suitable for high-power. applications, and PZT-5A and PZT-5H, representative of materials suitable for low power or detection service (hydrophones, etc.). These are all modified $Pb(Zr,Ti)0_3$ compositions just on the tetragonal side of the tetragonal-rhombohedral phase boundary. PZT-4 has about 5-at.% Sr^{2+} substitution for Pb^{2+}, and PZT-8 has about 5% Sr^{2+} substitution for Pb^{2+} and acceptor doping (three-valent atom in B position of perovskite $AB0_3$ lattice). PZT-5A and PZT-5H have donor doping (three-valent atom in A position or five-valent atom in B position).'

Several papers have appeared over the past few years on stress and field sensitivity of transducer ceramics. Notable among these is the continuing series from the Canadian Naval Research Establishment at Dart-

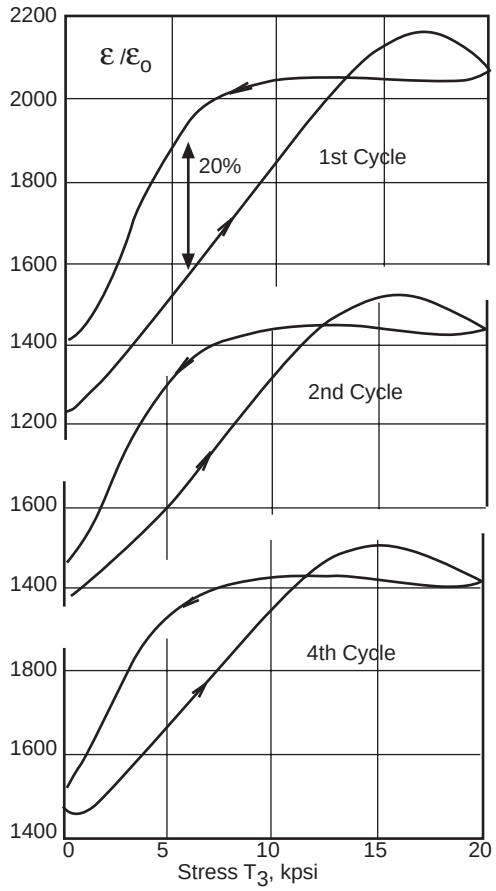

FIG. 1. ε33T/eo vs parallel stress TI for PZT-4; first, second, and fourth cycles.

mouth, Nova Scotia. The other continuing work (including this work) has been that done at the Elec-

tronic Research Division of Clevite Corporation. Russian and Japanese studies have also been done, but

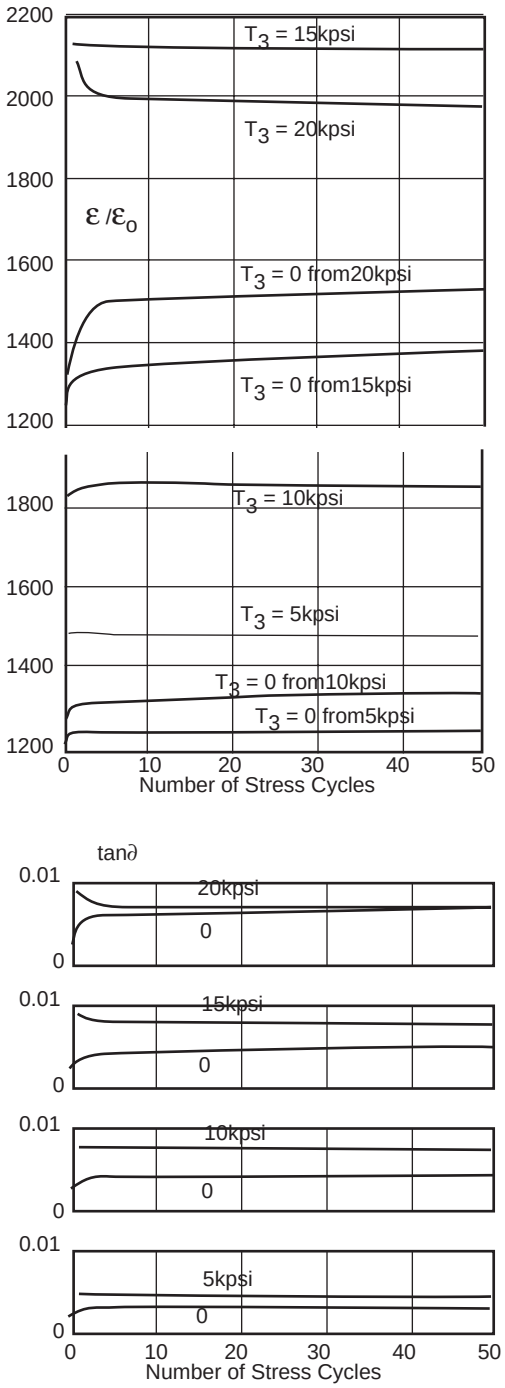

FIG. 2. ε33T/eo and tanθ vs number of stress cycles for peak stresses of 5, 10, 15, and 20 kpsi. PZT-4.

not on materials generally available in this country; and this work is therefore not referenced here.

This report is not presented as an analytic paper but as a descriptive technical report on piezoelectric materials. As such, it is largely a compendium of graphs, most of which are able to speak for themselves. Conclusions of a very general nature accompany the curves. Comments on measurement methods are found in the Appendix. Part 2 of this report describes an effective stabilizing treatment that markedly

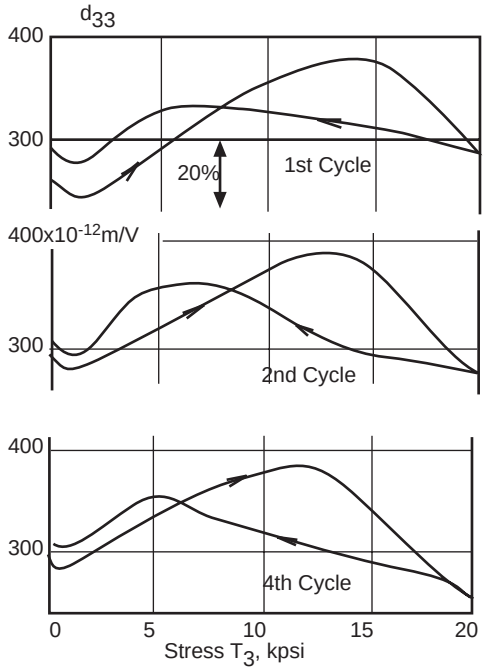

FIG. 3. d33 vs parallel stress T2 for PZT-4; first, second, and fourth cycles.

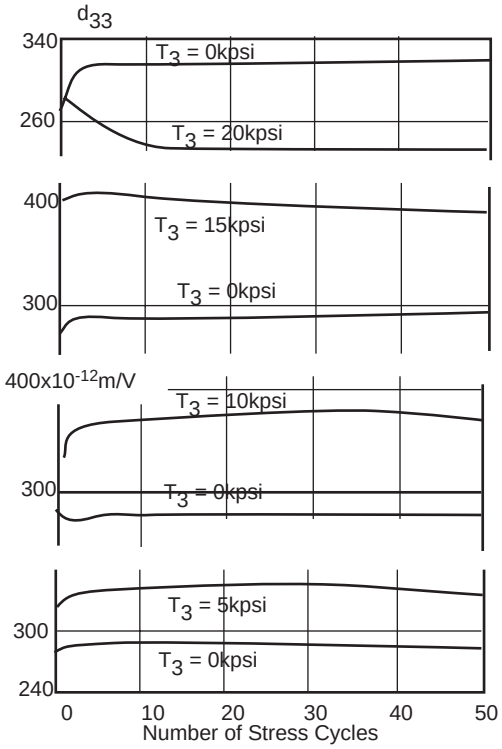

FIG. 4. d33 vs number of stress cycles for peak-stresses of 5, 10, 15, and 20 kpsi. PZT-4.

reduces variations of permittivity with compressive stress. Part 3 discusses effects of static compressive stress perpendicular to the polar was.

1. EXPERIMENTAL RESULTS

Specimens were exposed to static compressive stress parallel to the polar axis in cycles to 5, 10, 15, and 20 kpsi. For the materials capable of withstanding these high compressive stresses (PZT-4 and PZT-8), detail

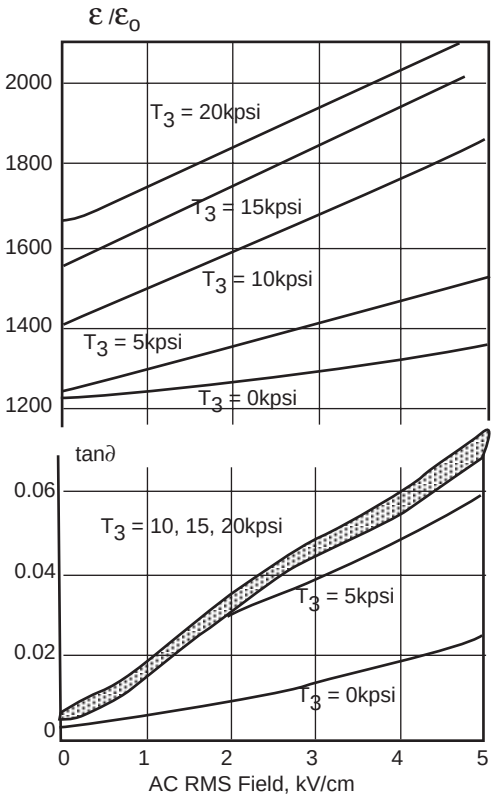

FIG. 5. $\varepsilon_{33}T/\varepsilon o$ and tanθ vs ac rms field at 0, 5, 10, 15, and 20 kpsi. PZT-4.

runs were made to 20 kpsi with the first, second, and fourth cycles. Thereafter, measurements were made every fifth cycle at the stress end points up to a total of 50 cycles. Stress cycling runs measuring properties at end points only were made at 5-, 10-, and 15-kpsi peak stress. This plan was varied for the PZT-5's where a lower stress series was used for the detail run, or additional detail runs were made at lower stresses. This stress regimen gives stress limitations of the ceramics. However, each designer would normally desire detail runs at his particular design stress, and knowledge of the effects of stress cycles to this value of stress. The above compromise provides enough information that good estimates can be made within the range of stresses.

The behaviour with increasing stress will be the same as the first detail run shown here, of course. The return to zero stress must be estimated. Generally, this return path will have less hysteresis than the path from full stress, and in rough proportion to the peak stress expected. Permittivity, tanθ and d_{33} were measured as a function of stress parallel to the poling axis (T_3). Measurements of permittivity and tanθ with combined static stress and high ac electric field were also made.

A. PZT-4

Figures 1-5 show the typical changes of properties for PZT-4 with parallel compressive stress (parallel here means parallel to the poling axis, stress T_3). The detail runs (Figs. I and 3) show large percentage FIG.

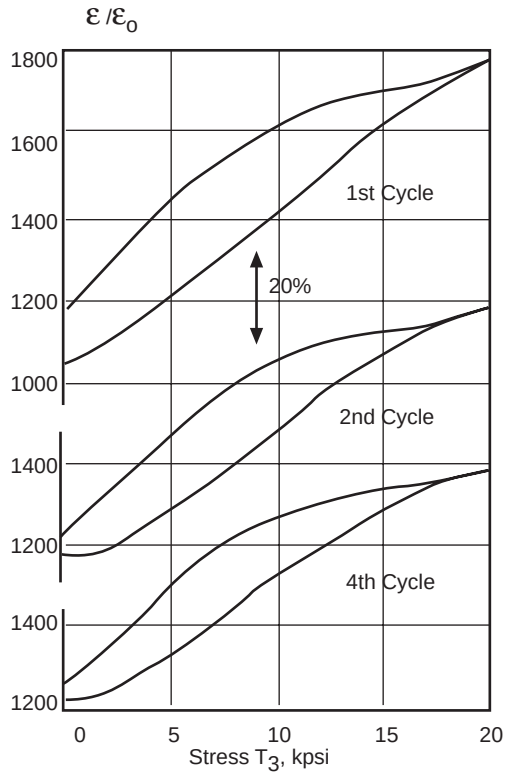

6. $\varepsilon_{33}T/\varepsilon o$ vs parallel stress T_3 for PZT-8; first, second, and fourth cycles.

changes of ε_{33} and d_{33} along with good recovery, in spite of fairly large hysteresis. The large change in $\varepsilon_{33}T$ with stress causes serious detuning of the tuning FIG.

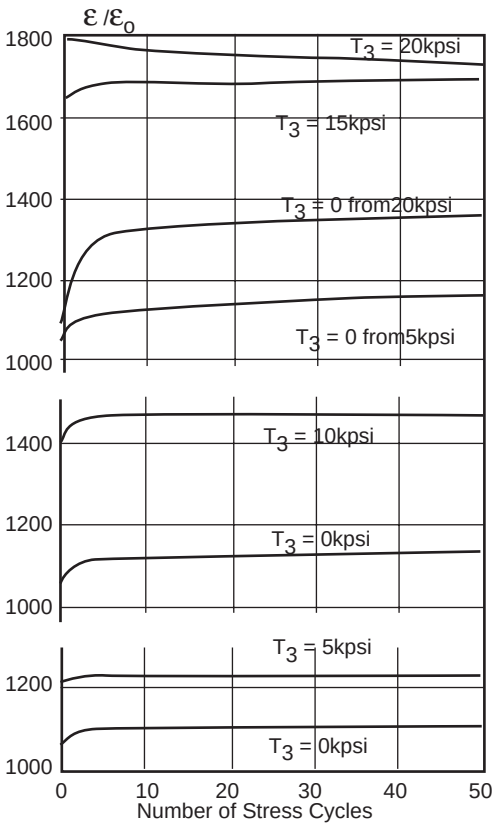

7. $\varepsilon_{33}{}^{T}/\varepsilon_o$ vs number of stress cycles for peak stresses of -5, 10, 15, and 20 kpsi. PZT-8.

inductance for high bandwidth transducers operating over -a good portion of this wide stress range. In most instances, retuning of the inductance is not possible. A small amount of stress stabilization is evident in Fig. 1, not so much by the reduction of the slope of the ε_{33}^{T}-vs-T curve, but the lowered stress of the ε_{33}^{T} peak and consequent reduction of hysteresis and total change. Thus, the maximum change during the first cycle is (2165-1230)/1230 = 76% with the peak at 16.5 kpsi as compared to (2120- 1460)/1460= 45% with the peak at

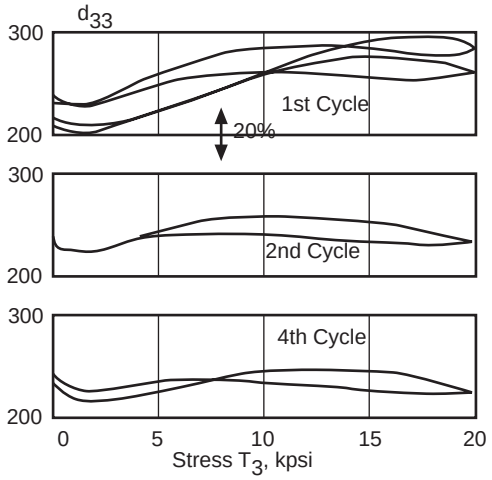

Fio. 8. d_{33} vs parallel stress T_3 for PZT-8; Erst, second, and fourth cycles.

15 kpsi for the fourth cycle. A further indication of stabilization can be found in the ε_{33}^{T}-vs-T_3 cycles curve (Fig. 2) that has end points only, showing that gross changes, cycle to cycle, cease after five or six cycles [10

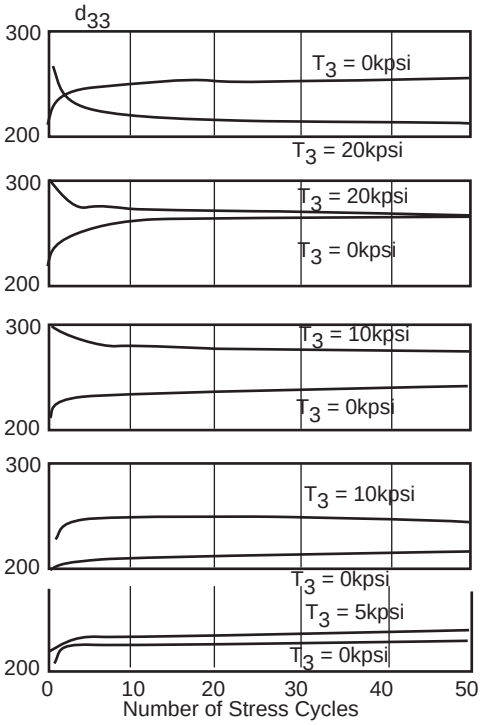

FIG. 9. d33 vs number of stress cycles for peak stresses of 5, 10,15, and 20 Lpsi. PZT-8.

cycles for d_{33} (Fig. 4)] to 5 or 10 kpsi. Note, however, that this "stabilization" is still continuing at 50 cycles at 20 kpsi with the change for ε_{33}^{T} between end points for this stress equivalent to about 29%. The continuing change in properties suggests that 20 kpsi is causing degradation and that PZT-4 should not be subjected to stress of this magnitude for applications requiring large numbers of cycles or long exposure times. Changes are, however, not catastrophic. Figures 2 and 4 show only minor changes from cycle to cycle for peak stresses of 10 and 5 kpsi. Note that the changes from zero to peak

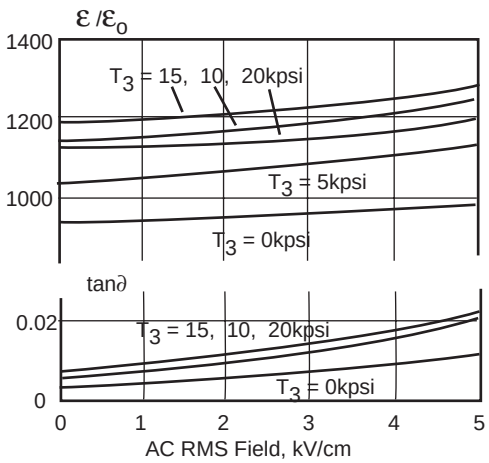

FIG. 10. $\varepsilon_{33}^{T}/\varepsilon_o$ and tand vs ac rms field at 0, 5, 10, 15, and 20 kpsi. PZT-8.

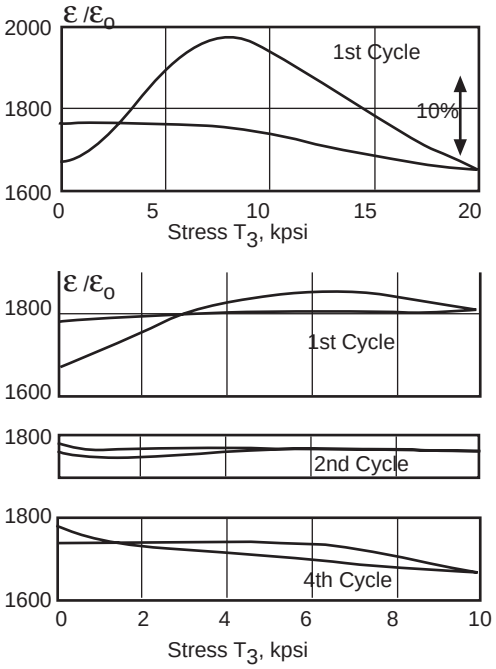

FIG. 11. $\varepsilon_{33}^{T}/\varepsilon_o$ vs parallel stress T_3 for PZT-5A; first, second, and fourth cycles.

stress are greatest for 15 kpsi, or the stress nearest the peal, for ε_{33}^{T} or d_{33}-vs-T_3 detail runs, and that there is little evidence for degradation at stresses at or below this value.

Figure 5 shows measured values of ε_{33}^{T} and tan∂-vs-ac field up to 5 kV/cm at various bias stress (parallel) levels for disks of 5:1 diameter-to-thickness ratio. A comparison at low-field levels with Fig. 1 shows clearly that the thin disks necessary for the high-drive work introduced much lateral clamping, preventing much of the rise in ε_{33}^{T} With T_3. Nevertheless, these data indicate the direction, and to some extent, the magnitude of the true changes with combined high ac electric field and parallel static stress, useful especially for comparison of materials. Using Figs. 1 and 5, one

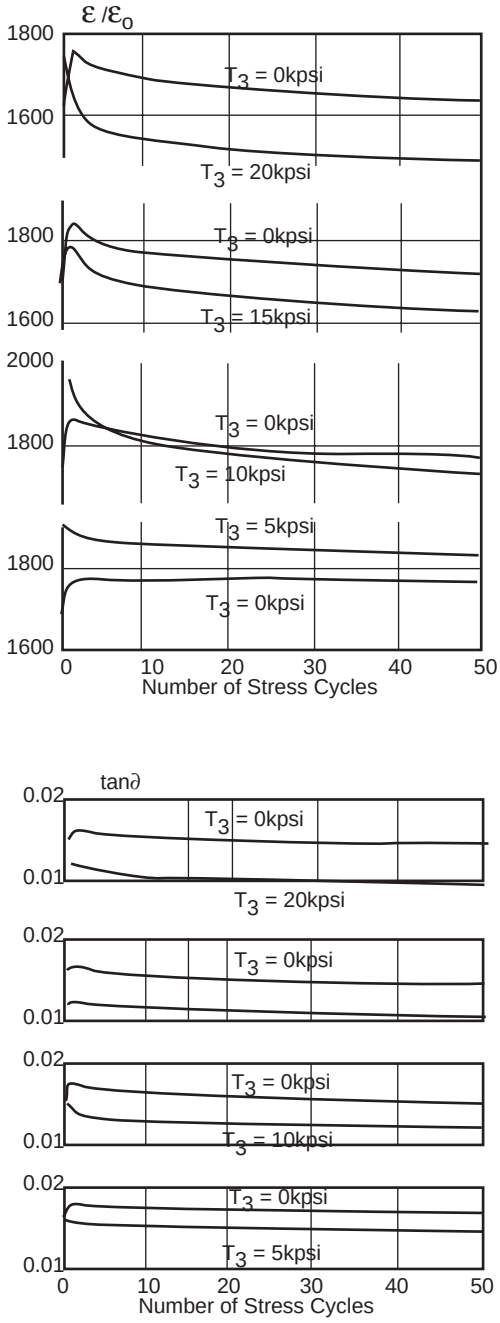

Fig. 12. $\varepsilon_{33}^{T}/\varepsilon_o$ and tans vs number of stress cycles for peak stresses of 5, 10, 15, and 20 kpsi. PZT-5A.

may extrapolate very roughly for a specific design case: Suppose one wants $\varepsilon_{33}^{T}/\varepsilon_o$ at 10 kpsi (T_3) and ac drive of 3 kV/cm rms. $\varepsilon_{33}^{T}/\varepsilon_o$ at low field is 2050 from Fig. 1, and has increased owing to the electric field from 1400 to 1680 from Fig. 5. So, this extrapolation gives the relative permittivity, for the specified conditions as [(1680/1400) 2050]=2460. A similar extrapolation could be made, probably with less justification,_ for tan∂. From tan∂ data taken with the permittivity data of Fig. 1, this would raise tan∂ of Fig. 5 to 0.064 from 0.047.

As mentioned in the Appendix, this sort of extrapolation is probably very inaccurate at stresses over the peak in ε_{33}^{T} vs T_3 (Fig. 1) since the high-drive data do not show a corresponding peak. Tan∂ figures of Fig. 5 reflect the very low initial value of tan∂ for the particular specimens used and should be modified in any specific case by the data in Fig. A-1 of the Appendix, which shows high drive results for specimens of different initial tan∂. Aging reduces tan∂, of course, so improved tan∂ vs driving field will accrue naturally with time. Exposure to high ac fields and/or high static stress will, however, act to raise the value of tan&; note Fig. 1. We may interpret this as a "de-aging" effect. Any large mechanical, electrical, or thermal signal will act to institute a new aging cycle.

B. PZT-8

This composition was developed especially for highpower applications. It is outstanding in regard to smaller changes in tan∂ and permittivity at high ac drive levels. Piezoelectric properties are reduced com

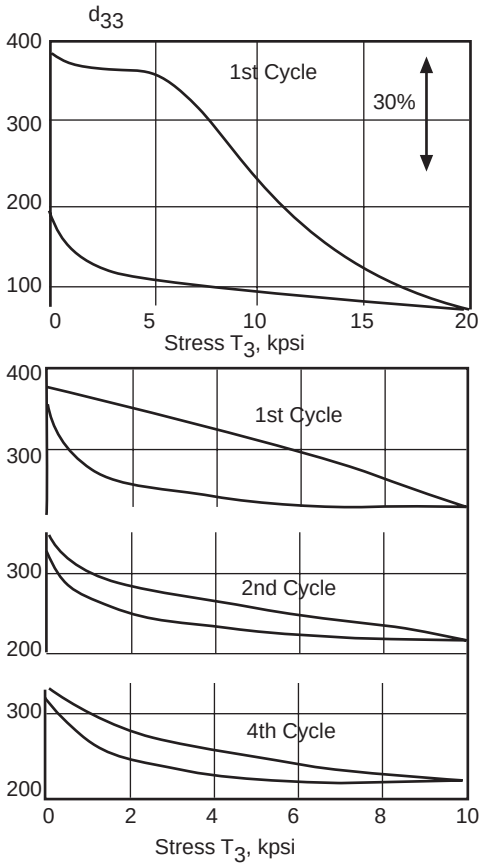

FIG. 13. d_{33} vs Parallel stress T_3 for PZT-5A; first, second, and fourth cycles.

pared to PZT4, but not seriously. Additional benefits of this modified composition are demonstrated in Figs. 6-10, where effects of parallel stress on properties of PZT-8 are displayed. The ε_{33}^{T} vs T_3 curves in Fig. 6 show that with PZT-8 there is no peak below 20 kpsi; otherwise its behavior is similar to that of PZT-4, but with markedly lower slope. The solid dots-represent an early production run of PZT-8, while the open circles are for an even earlier pilot plant batch. The curves drawn represent an average between the lots. For the first cycle, the maximum change is (1780-1053)/1053 =6976 - not a great improvement over PZT-4; but at the stress at which PZT-4 would peak, the change with PZT-8 is (1675-1053)/1053 = 59%, an appreciable improvement over the 76% change for PZT-4. There is also a degree of stress stabilization: The fourth cycle in Fig. 6 shows an average change for the two pairs of specimens of (1780 - 1230)/1230 = 45%, the same as f or PZT-4, but again, the change is spread over the entire 20-kpsi stress range, whereas with PZT-4, this change occurs in the range to 15 kpsi where the curve peaks.

PZT-4 and PZT-8 can be compared further; Fig. 2 with Fig. 7, and Fig. 4 with Fig. 9. Stress stabilization

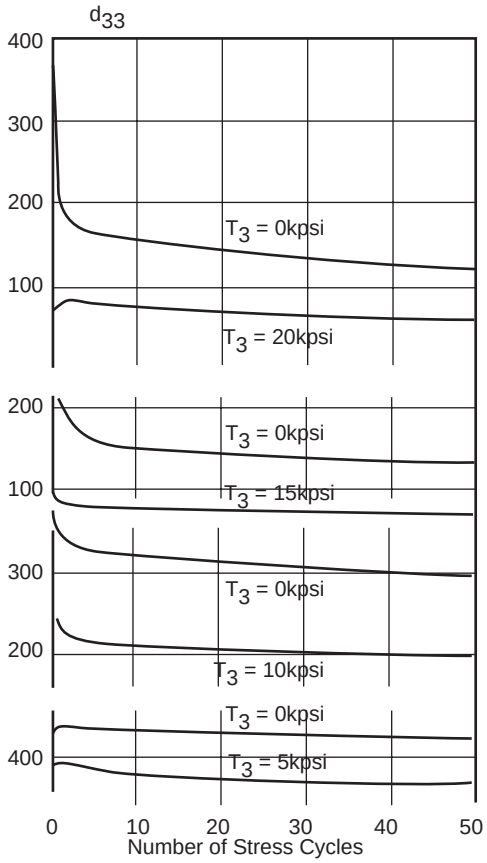

FIG. 14. d33 vs number of stress cycles for peak stresses of 5, 10, 15, and 20 kpsi. PZT-5A.

has been completed to a large extent after 10 stress cycles. For the stress range to 5 kpsi, ε_{33}^{T} increases about 19% for PZT-4 and 11% for PZT-8, with little difference between 10 and 50-cycle end-point values, The corresponding changes in d_{33} are about + 19% and +3%, respectively. The divergence between the 10th and 50th cycle has increased slightly for the 10-kpsi stress range, but is significant for the 15-kpsi stress range. For the latter stress, the rise in $\varepsilon_{33}T$ is 58% for the 10th and 54% for the 50th cycle for PZT-4; 49% for the 10th and 37% for the 50th stress cycle for PZT-8. The changes in d_{33} are +42% for the 10th and 34% for the 50th cycle for PZT-4 21% for the 10th and 14% for the 50th cycle for PZT-8. On the other hand, the divergence between the 10th and 50th cycle is again very small for the 20-kpsi stress range, with rise in $\varepsilon_{33}T$ of +23% and +300/0 for PZT-4 and PZT-8, respectively, after the 10th cycle. Note that the change in d_{33} is now negative, however; about -25% for PZT-4 and about -15% for PZT-8 (pilot plant lot) beyond 10 cycles. These facts suggest a stress-induced degradation mechanism that initiates around 15 kpsi (since changes are continuing at 50 cycles) and that is essentially completed alter 10 cycles at 20 kpsi. As a practical matter, this further suggests rough stress limits below 15 kpsi for PZT-4 and PZT-8 when progressive

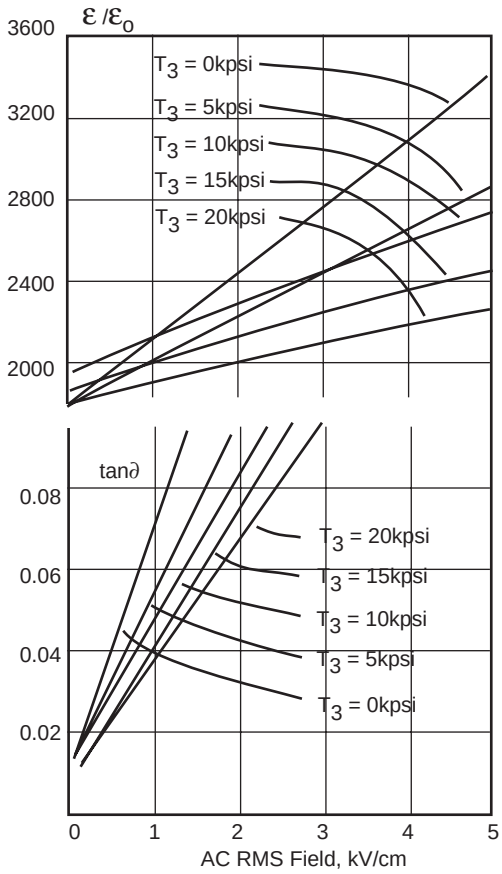

FIG 15, $\varepsilon_{33}T/$to and tanδ vs ac rms field at 0, 5, 10, 15, and 20 kpsi. PZT-5A.

changes in properties with stress cycling must be avoided. The permanence of the stress stabilization that occurs above 15 kpsi has not been checked and remains open for further fruitful study.

Figures 8 and 9 show the sensitivity of d_{33} to parallel stress for PZT-8. There is sufficient difference in the two lots to warrant plotting both. Note that the early

production lot (solid dots) in Fig. 8 rises more with stress than the pilot plant lot. In Fig. 9, the stresscycles run for the 20-kpsi case has been drawn for both lots and indicates that this rise in d_{33} is maintained to some extent out to 50 cycles, where d_{33} for the pilot plant lot falls below the no-stress value after the second cycle. Neither case shows as large a change in d_{33} with T_3 as PZT-4.

It is known, of course, that the high-drive properties of PZT-8 are superior to those of PZT-4 at low stress, and, in fact, PZT-8 was specifically developed with this as a goal (with due consideration for practical and useful levels of $\varepsilon_{33}T$ and electromechanical coupling). The superiority at high stress is, nevertheless, remarkable (see Fig. 10 compared to Fig. 5), considerably greater

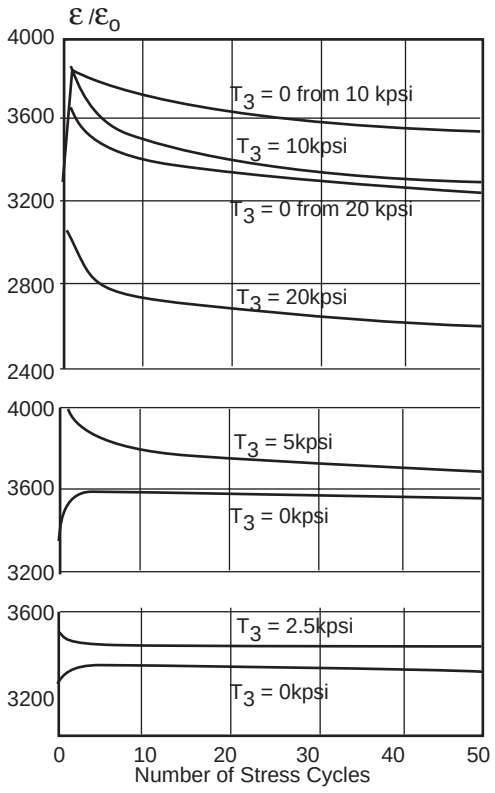

Fig. 16, $\varepsilon_{33}T/\varepsilon_o$ vs number of stress cycles for peak stresses of 2.5, 5, IT, and 20 kpsi. PZT-5H.

than at low stress. Here, too, lateral clamping must cause some error in the values, probably about the same as for PZT-4. One can perform the same extrapolation as was done for PZT-4; $\varepsilon_{33}T$ and tan∂ for 10 kpsi and 3 kV/cm: For $\varepsilon_{33}T$, (1620)(1190)/1140=1690; for tan∂ (not shown in Fig. 6), 0.014 to 0.011, which is lower than Fig. 10 shows because of the unusually low tan∂ at 10 kpsi for the specimens of Fig. 6. The conservative approach is to take the higher figure (0.014). Another comment on the PZT-8 high-drive data of Fig. 10 is that a peak of $\varepsilon_{33}T$-vs-T_3 is indicated for these partially clamped samples since the 20-kpsi curve lies below the 10- and 15-kpsi curves; this does not appear in the data for the pairs of cubes (Fig. 6) that are much closer to the laterally free case. Thus, both PZT-4 and PZT-8 high-drive curves contradict the $\varepsilon_{33}T$ vs T_3 runs made at low driving fields. It is apparent that combination of hydrostatic and axial stress, as actually occurs with comparatively thin specimens on compression, is considerably more favorable than axial stress alone, especially with PZT-8. This has practical significance for transducer design. It is not difficult to arrange for such a situation with stiff loading and backing masses or stiff inserts between ceramic elements in a stack.

C. PZT-5A

PZT-5A is a donor-doped lead titanate-lead zirconate solid solution for which the doping increases the

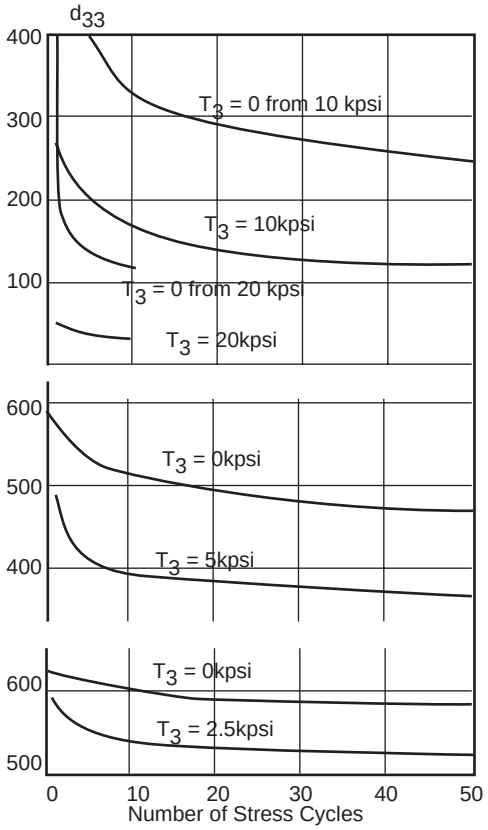

Fig. 17. d_{33} vs number of stress cycles for peak stresses of 2.5, 5, 10, and 20 kpsi. PZT-S5.

domain mobility to the point where the structure quickly adjusts itself to external influences and remains relatively relaxed. This results in low aging rates, high couplings, and easy poling, Unfortunately, the high domain mobility also results in easy stress or field depoling, and high dielectric and mechanical losses, particularly at high ac fields. The upper curves of Figs. 11 and 13 indicate drastic degradation of polarization at stresses above 8 Ipsi. Therefore, the stress regimen was followed with detail runs at only 10 kpsi, and the remainder of Figs. 11 and 13 are devoted to these. The relative stability of $\varepsilon_{33}T$ with stress may be interpreted as a fortuitous combination of circumstances. Domain alignment changes due to stress act to increase $\varepsilon_{33}T$ as with PZT-4 and PZT-8, but extreme domain mobility in the donor-doped material

is partially and progressively clamped by stress. This is further reinforced by the high-drive data of Fig. 15 compared to Figs. 5 and 10, which show that permittivity changes are less with stress for the donor-doped PZT-5's, and that tan∂ actually decreases with stress. With the PZT-4 and PZT-8, stress clamping is less effective than generation of new domain walls with stress and their contribution to permittivity and loss. In spite of the favorable effect of stress in reducing dielectric loss in the donor-doped ceramics, the losses remain too high to allow serious competition with PZT-4 or PZT-8 when efficiency as a driver is required.

Figures 13 and 14 show that no maintained stress or stress cycle leaves the ceramic unaff ected, but the degradation is modest at 5 kpsi and up to 10 kpsi if the stress is not cycled. An important distinction that must be made is that with -the non-donor-doped materials there is stabilization after a few stress cycles below 15 kpsi. With the donor-doped materials, this is not the case; continued degradation occurs even after 50 cycles. It is noteworthy, however, that with stress maintained, the donor-doped materials behave rather well; aging is in fact markedly less pronounced than with the non-donor-doped ceramics (see Ref. 15). These characteristics are all consistent with the introductory statement on domain mobility above.

D. PZT-5H

The data for PZT-5H, another donor-doped material, are summarized in Figs. 16 and 17. All remarks concerning PZT-5A hold even more emphatically for PZT-5H. Therefore, the stress cycles runs were made to 20,910, 5, and 2.5 kpsi. Even the 2.5-kpsi cycles run (Fig. 17) shows degradation, albeit modest enough for the ceramic to be quite useful. The forte of this composition is its unusually high ε_{33}^{T} and d_{33}. Even after an accidental or emergency exposure to 10 kpsi, the curves of Fig. 17 show that PZT-5H would recover to the extent that its d_{33} would remain over 400 $x10^{-12}$ m/V, which is better than any of the others with no stress exposure. So, in spite of its stress sensitivity, it is extremely valuable as a hydrophone transducer material.

The curves for the high-drive characteristics of PZT-5H under various bias stresses are not shown. It is eminently unsatisfactory under both conditions, and worse than PZT-5A. As with PZT-5A, stress acts to reduce changes of permittivity and increase in dielectric loss with ac electric field. Behavior under high electric .drive, nevertheless, remains very poor. This material cannot be recommended as a radiating transducer material.

ACKNOWLEDGMENTS

Support of the Office of Naval Research is gratefully acknowledged. We are indebted to Dr. Paul Smith of the Naval Research Laboratory for discussion and moral support and to Don Berlincourt and Bernard Jaffe for critical review of the manuscript. James Peterson was invaluable in developing several of the measurement techniques and performed many of the experiments. Other measurements were made by Donald Lellis and Bennie Cohran. Specimen preparation was done by the Electronic Research Division Pilot Plant under Fred Salasek.

Appendix A: Measurement Techniques

I. ε_{33}^{T}/ to vs T_3 AND ASSOCIATED tan∂

Specimens were 1/2in. cubes, carefully chosen to have similar initial tan∂, ε_{33}^{T}, and d_{33}. Figure A-1, showing tan∂-vs-T_3 for specimens of PZT-4 of different initial tan∂, shows dearly the tendency for the specimens to maintain their relative positions and, therefore, the need for uniform samples. samples were lapped- on all faces, plane and parallel to well within 0.2%. The piezoelectric constant d_{33} was measured for all specimens in a group and matched pairs were used for each measurement. The two were placed between platens of a Dillon Universal tester with hardened steel anvils transfering the stress to the specimen, with a half-ball and socket leveller incorporated into one of the anvils. The specimens were driven out of phase so that the piezoelectric forces generated would not excite resonances in the press. Single-cube experiments invariably yielded frequency-dependent loss peaks in the tan∂-vs-T_3 curves. Capacitance and dielectric loss were measured with a GeneralRadio 716-C bridge at 1 kHz and a few volts (definitely a low field for these specimens). Stresses were changed stepwise with a 1-min wait after each desired stress was reached before readings were taken. Detail runs were taken in this fashion for the first, second, and fourth stress cycles, generally to a peak stress of 20 kpsi. Thereafter, the cycling was continued in a nonstepwise fashion with measurements being made at zero and peak stress (initial, peak, and final) every fifth cycle up to a total of 50 stress cycles. These m measurements are assumed to be accurate with the exception of some lateral clamping of the specimens due to the press anvils and the out-of-phase lateral piezoelectric clamping between the stacked cubes. Both effects are thought to be quite small.

II. $\varepsilon_{33}^{T}/\varepsilon_3$ vs E_3 AT VARIOUS T_3 AND ASSOCIATED tan∂

Because of the voltage limitations of the GR 716-C capacitance bridge, thin specimens (5-mm-diamx 1-mm thick disks) were used. They were again driven out of phase in pairs. Here lateral clamping is quite severe, as the low-field comparison between measurements on the cubes and the disks shows (Fig. A-2). As mentioned in the text, except at $T_3 = 0$ this measurement is a comparative one only, and does not show the true extent of the changes in ε and tan∂ with stress at high field. For quantitative results, at the very least, the field-variable data must he multiplied by the ratio of values found for the cubes to values found for the disks at low fields, and this

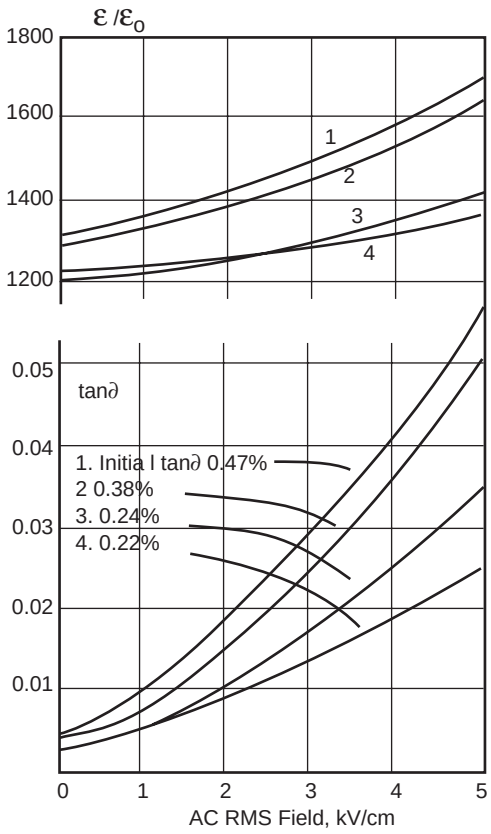

FIG. A-1. $\varepsilon_{33}^{T}/\varepsilon_o$ and tans vs ac rms field for PZT-4 specimens of different initial tan∂

extrapolation is doubtless limited for e to the peak that occurs with PZT-4 (and the PZT-5's on the first cycle) as function of stress, and not beyond. The extrapolation has very limited reliability in any case. An extra precaution was taken for these high-drive measurements owing to the fact that nonlinearities result in generation of second harmonics dependent on tan∂. More filtering than the G-R null detector provides was necessary to prevent the bridge balancing on the second harmonic or some vague average of fundamental and second harmonic that invariably gives lower than the correct tan∂. Good results were also critically dependent on good electrodes; evaporated gold was found satisfactory.

III. d_{33} vs T_3

The piezoelectric strain-field constant d_{33} was measured by a strain-gauge technique. Metal-foil gauges were bonded to the 1/2-in. cube specimens using short gauges so as not to short circuit the ceramic or permit arcing through the gauges by the driving field. Eastman 910 cement was found to be a convenient bonding agent. Stacked specimens driven out of phase were used, as for the dielectric measurements, The applied driving voltage was roughly inversely proportioned to the d constant being measured, typically 500 V rms for PZT-4. This gives a strain of about 12X 10-6 rms. The detection was made with a 1-kHz carrier bridge, roughly balanced statically, with the 100Hz dynamic signal measured at one of the sidebands (900 or 1100 Hz) to avoid measurements at the driving frequency. The carrier voltage was

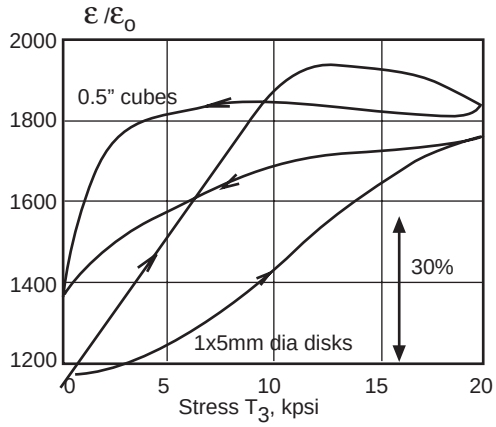

FIG. A-2. $\varepsilon_{33}T/\varepsilon_o$ vs parallel stress T3 for PZT4 cubes compared to disks.

generally set at 5 V rms. Because some of the ceramics depolarize seriously under high stress, it was imperative to ascertain in each instance whether this was truly the case if the measurements showed it, or whether the measuring gauge had loosened. This was done by measuring the d constant independently before and after the stress cycling on a speaker-drive d meter. This instrument applies a calibrated dynamic (100 Hz) stress of about 1 N to the test elements. Its output into a large capacitor gives

$$d_{33}=\partial D/\partial T_E = \partial S/\partial E_T$$

If the two methods did not give comparable d constants, it was assumed that something had happened to the strain gauge. To measure the microvolt signals generated in the strain-gauge method, a Hewlett-Packard model 302A wave analyzer was used. For a symmetrical strain-gauge bridge (dummy resistance equals activegauge resistance),

$$\text{STRAIN S (rms)} = \frac{4\sqrt{2}\ \text{SIDEBAND VOLTAGE}}{\text{GAUGE FACTORxBRIDGE VOLTAGE}}$$

where the field

$$\text{E (rms)} = \frac{\text{SPECIMEN DRIVING VOLTAGE (rms)}}{\text{SPECIMEN THICKNESS}}$$